 DOI:10.3217/978-3-85125-378-8-44

Training Free Error-Potential Detection

Matthew Dyson[1], Emmanuel Maby[2], Laurence Casini[1], Margaux Perrin[2], Jérémie Mattout[2] and Boris Burle[1]

[1] LNC, UMR7291, Aix-Marseille Université, CNRS, Marseille, France
matthew.dyson@univ-amu.fr, laurence.casini@univ-amu.fr, boris.burle@univ-amu.fr
[2] INSERM U1028, CNRS UMR5292, Lyon Neuroscience Research Center, Bron, France
manu.maby@inserm.fr, margaux.perrin@inserm.fr, jeremie.mattout@inserm.fr

Abstract

Error potential detection systems typically have to be trained on each individual, often necessitating that users experience sub-optimal active system performance. In this work, by introducing neurophysiological knowledge to preprocess EEG, we present a training-free error potential detection system. Results demonstrate that a subset of error potentials may be discriminated with a high level of precision in previously unseen subjects.

1 Introduction

Passive error potential (ErrP) detectors may be utilised to correct or negate the output of active BCI systems, providing output verification. Coupling active and passive BCI systems can increase training requirements. In this analysis we demonstrate an approach which generalises information across subjects, allowing poor BCI performance by some subjects to aid other users.

The underlying EEG component of ErrP detection systems is feedback related negativity (FRN). Key features of FRN make it a primary candidate for the reinforcement learning (RL) theory of error feedback, since it is thought to originate from the anterior cingulate cortex (ACC) [6], and to be triggered by phasic changes in dopaminergic signals from the basal ganglia [3]. In our method neurophysiological knowledge is used to inform projection filters, which perform joint dimensionality and noise reduction [1]. In RL theory, error trials will not necessarily exhibit FRN, therefore we only target a subset of trials using precision based loss functions [4].

2 Method

2.1 Data

Results from two BCI datasets are presented - detailed descriptions are available for both [2, 5].

The development data set, acquired in Marseille, consisted of 64 channel EEG recorded using a Biosemi Active2. Eleven subjects performed online motor imagery sessions using a Graz protocol modified to display discrete feedback. Subjects performed four runs of 40 trials. Three feedback periods were embedded in each trial. Feedback was manipulated to ensure all subjects experienced minimum error rates of 20%. Data from two subjects was rejected. After artefact removal the average error rate was 23±2%. We refer to this data as the MI set. A second data set, acquired in Lyon was recorded with 56 EEG sensors using a VSM-CTF compatible system. This analysis is based on 32 electrodes. Sixteen subjects used a pseudorandom stimulation procedure P300-speller. Flash duration and stimulus onset asynchrony parameters were selected to increase the difficulty of spelling. Each subject performed four 12 minute spelling sessions, a session consisted of 12 five letter words with feedback for each letter. After artefact rejection the average error rate was 30±19%. Four subjects with a error rate below 10% after artefact rejection were not included in this analysis. This data will be referred to as the P300 set.

2.2 EEG Preprocessing

EEG data was bandpass filtered between 3 and 12 Hz using 4th order Chebyshev filters. Source time series were obtained using transformation matrices designed for real time use [1]. Applied to EEG, these matrices output x, y and z current triplet for each of the voxels in the LORETA head model. Voxels belonging to Brodmann areas 24, 32, 33, 8 or 6 were included in a fixed region of interest (ROI), encompassing all FRN activation foci described in meta analysis [6]. The radial, z, value of all voxels in the ROI were averaged to create a single virtual channel, of sample rate equal to surface channels, on which all further analysis / processing was performed. Using this approach, the virtual channel retains a proxy to polarity observed in central channels.

2.3 Feature Space

Training data was generated for each subject using data from others in the same set. Each subject's virtual channel amplitude was normalised by the standard deviation. Subject's virtual channel ERPs were aligned to the median FRN latency of the group, the *normalised latency*, by circular shifting of trial values and peak alignment. A template error FRN was derived from the average of the normalised error trials. Three features were then extracted from a window around the normalised latency. *Amplitude* measured peak negativity within the window. *Jitter* measured the distance between peak negativity and the normalised latency. *Similarity* measured correlation between single trial activity and the template error FRN when accounting for *Jitter*.

2.4 Classifier Calibration

SVM$^{\text{perf}}$, a classification method for multivariate performance measures [4], was trained on the feature space. A radial basis function kernel and a precision/recall breakeven point loss function were used. SVM parameters cost, C, and gamma, g, were obtained through grid search. At each search step nested 2×10 cross validation was performed and an F-score obtained from rates of precision and sensitivity. The C and g pair which maximised F_β was selected. For P300 calibration five of 12 subjects were excluded from training data (the *hold-back* group) after visual inspection of virtual channel data suggested they had few discriminable error trials.

2.5 Online Steps

As subject independent classifiers were calibrated on amplitude and latency normalised feature spaces, online calculations required equivalent distributions. Amplitude normalisation in online steps was based on estimates of statistical moments, updated on a trial by trial basis, using parameterless one pass methods described by Terriberry [7]. Temporal normalisation of the feature space required an estimate be made of each new subject's FRN latency without use of class labels. Latency was tracked via estimation of how a temporal window of activity influenced the *Similarity* feature. A moving average, $\widehat{Similarity}$, was maintained on a trial by trial basis:

$$\widehat{Similarity}_t = Similarity.UC + \widehat{Similarity}_{t-1}.(1 - UC) \quad (1)$$

The update coefficient, UC, was bounded between 0 and 0.1. The seed, $\widehat{Similarity}_0$, was set to perfect correlation with mean training error FRN, scaled by a mid-range UC value of 0.05. As *Similarity* was invariant to magnitude, UC was weighted by trial amplitude data in order to only update $\widehat{Similarity}$ on trials exhibiting negative polarity in the period of interest:

$$UC = 0.1/1 + e^{13(Amp+0.5)} \quad (2)$$

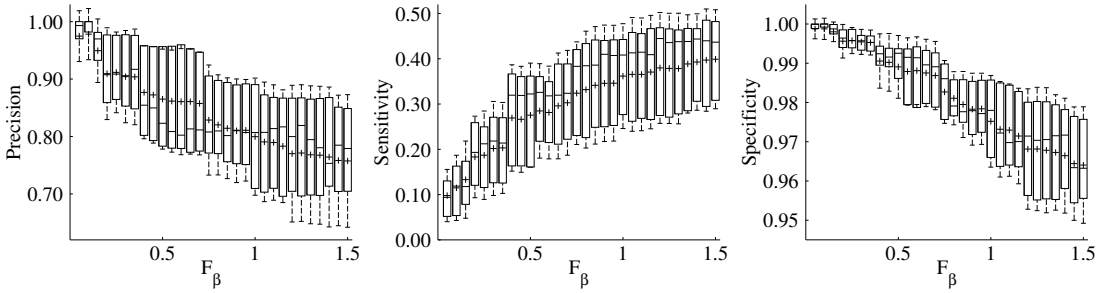

Figure 1: Error detection rates for MI dataset. Influence of F_β selection on overall group rates of precision, sensitivity and specificity. Results calculated from 50 simulation runs for each subject. Whiskers indicate standard deviation. Plus symbol indicates the mean.

Amp being the mean normalised amplitude in a window around the *normalised latency* for the trial. After each trial the estimate of FRN latency, $\widehat{Latency}$, was set to the trial period estimated to be most similar to the template error FRN:

$$\widehat{Latency} = t \mid_{max(\widehat{\mathbf{Similarity}}_t)} \tag{3}$$

After amplitude normalisation, *Amplitude*, *Jitter* and *Similarity* features were extracted from a window centred on $\widehat{Latency}$ and trials classified by SVM. An additional step detected ERP polarity inversion. Polarity inversion may occur due to differences in sulci orientation and the relative position of dipoles. This step was based on sequential calculation of the third central moment and the standard error of skewness. If significant positive skew was detected at $\widehat{Latency}$, data was deemed inverted and the polarity of all succeeding trials reversed.

3 Results

Figure 1 shows the influence of the F-score β on ErrP detection rates for the MI dataset; demonstrating that overall precision can be increased at the cost of sensitivity and specificity. Further results are based on a β value of 0.5, corresponding to the typical $F_{0.5}$ measure weighting precision over sensitivity. Post-hoc comparisons were performed on the MI development dataset to verify contributions of the method. Paired t-tests showed source based preprocessing provided better sensitivity (M=27.1, SD=11.5) than equivalent use of monopolar (M=19.7, SD=15.0, t=-3.23, p=0.012); laplacian (M=16.9, SD=16.1, t=-3.75, p=0.006); and surface spline (M=21.9, SD=15.5, t=-2.47, p=0.039) time series from sensor channel FCz. Use of FRN latency tracking produced significant (t=-2.78, p=0.024) improvement in sensitivity rates (M=27.3, SD=11.4) in comparison to use of a fixed value set to the normalised latency (M=23.6, SD=11.2).

Individual ErrP detection rates are detailed for both the MI and P300 datasets in Table 1. P300 subjects in the *hold-back* group obtain poor overall results, with mean precision, sensitivity and specificity of 38.6±27.4, 5.6±30 and 96.1±3.6. Mean rates for precision, sensitivity and specificity for the seven remaining subjects in the P300 dataset were 86.9±15.3, 21.4±17 and 98.2±1.9. Post-hoc analysis of the properties of these two groups showed the *hold-back* group had a reduced overall difference in surface EEG amplitude between feedback classes, as measured by subtracting correct trial average from error trial average at channel Cz, however this difference was only marginally significant following a one tailed hypothesis test (Welch's t, t=-1.8785, p=0.049).

	MI Data				P300 Data			
	Prec.	Prec. δ	Sens.	Spec.	Prec.	Prec. δ	Sens.	Spec.
S1	80.0±5.4	+59.3	10.8±1.2	99.3±0.2	*9.3±12.3*	*-28.7*	*2.2±3.0*	*89.9±0.8*
S2	95.6±1.4	+68.7	42.2±1.8	99.3±0.4	85.1±1.9	+49.4	42.5±3.5	95.9±1.1
S3	83.8±6.2	+61.3	17.6±1.8	99.0±0.3	92.7±3.0	+29.6	10.5±1.1	98.5±0.3
S4	93.2±1.6	+69.1	33.4±2.4	99.2±0.5	99.9±0.8	+44.9	16.7±1.0	100.0±0.3
S5	97.0±2.8	+74.1	32.1±2.2	99.7±0.5	*11.5±23.7*	*-16.3*	*0.9±1.9*	*98.5±0.4*
S6	77.4±5.1	+55.9	12.3±1.5	99.0±0.3	99.0±6.9	+39.6	0.8±0.7	100.0±0.2
S7	95.9±2.6	+75.5	35.9±3.1	99.6±0.6	*57.5±5.7*	*+33.3*	*18.5±1.8*	*95.5±0.4*
S8	79.3±6.2	+53.2	23.7±5.9	97.9±1.3	62.3±3.6	+49.4	47.1±3.3	95.8±0.4
S9	77.4±4.7	+57.7	36.8±2.6	97.4±0.5	69.8±6.3	+41.9	14.3±1.6	97.5±0.4
S10					99.5±2.7	+56.8	18.1±3.1	99.9±0.9
S11					*44.0±18.3*	*-2.1*	*1.7±0.7*	*98.2±0.3*
S12					*70.5±5.3*	*+39.1*	*9.9±2.0*	*98.1±0.5*
μ	86.6±8.6	+63.9	27.2±11.5	98.9±0.8	66.8±31.9	+28.1	15.3±15.4	97.3±2.8

Table 1: Error-potential detection rates for MI and P300 data sets. Precision δ denotes difference between precision obtained and equivalent randomisation of true label distributions. *Italics* denote members of the *hold-back* group. Results obtained using β value of 0.5. Simulation runs were repeated 100 times.

4 Conclusion

Discrimination rates demonstrate that strong neurophysiological a priori, with inverse solution methods to apply them, can produce viable training free approaches for ErrP detection. Signal enhancement provided by inverse methods can enable use of simple descriptive interpretable features.

5 Acknowledgments

This work was carried out as part of the CoAdapt project, funded via ANR-09-EMER-002-01.

References

[1] M. Congedo. OpenViBE tools. `http://sites.google.com/site/marcocongedo`, 2011.

[2] M. Dyson, L. Casini, and B. Burle. Discrimination of discrete feedback during performance of motor imagery. In *Proc. Int. Workshop on Pattern Recognition in NeuroImaging*, pages 93–96, 2012.

[3] C. B. Holroyd and M. G. H. Coles. The neural basis of human error processing: Reinforcement learning, dopamine, and the error-related negativity. *Psychological Review*, 109(4):679–709, 2002.

[4] T. Joachims. A support vector method for multivariate performance measures. In *Proceedings of the 22nd International Conference on Machine Learning*, pages 377–384. ACM Press, 2005.

[5] M. Perrin, E. Maby, S. Daligault, O. Bertrand, and J. Mattout. Objective and subjective evaluation of online error correction during P300-based spelling. *Adv. in Human-Computer Interaction*, 2012.

[6] K. R. Ridderinkhof, M. Ullsperger, E.A. Crone, and S. Nieuwenhuis. The roles of the medial frontal cortex in cognitive control. *Science*, 306:443–447, 2004.

[7] T. B. Terriberry. Computing Higher-Order Moments Online. `http://people.xiph.org/~tterribe/notes/homs.html`, 2007.